Accepted Manuscript

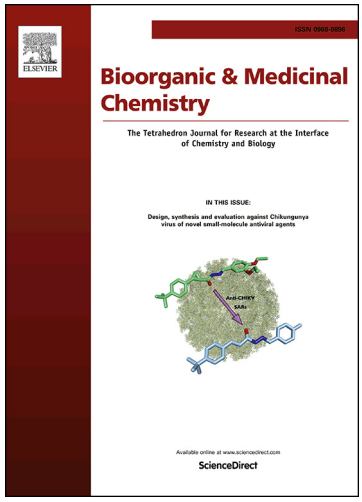

Multifunctional 5,6-dimethoxybenzo[*d*]isothiazol-3(2*H*)-one-*N*-alkylbenzylamine derivatives with acetylcholinesterase, monoamine oxidases and β-amyloid aggregation inhibitory activities as potential agents against Alzheimer's disease

Rui Xu, Ganyuan Xiao, Yan Li, Hongyan Liu, Qing Song, Xiaoyu Zhang, Ziyi Yang, Yunxiaozhu Zheng, Zhenghuai Tan, Yong Deng

PII: S0968-0896(17)32490-2
DOI: https://doi.org/10.1016/j.bmc.2018.02.037
Reference: BMC 14223

To appear in: *Bioorganic & Medicinal Chemistry*

Received Date: 24 December 2017
Revised Date: 7 February 2018
Accepted Date: 20 February 2018

Please cite this article as: Xu, R., Xiao, G., Li, Y., Liu, H., Song, Q., Zhang, X., Yang, Z., Zheng, Y., Tan, Z., Deng, Y., Multifunctional 5,6-dimethoxybenzo[*d*]isothiazol-3(2*H*)-one-*N*-alkylbenzylamine derivatives with acetylcholinesterase, monoamine oxidases and β-amyloid aggregation inhibitory activities as potential agents against Alzheimer's disease, *Bioorganic & Medicinal Chemistry* (2018), doi: https://doi.org/10.1016/j.bmc.2018.02.037

Multifunctional 5,6-dimethoxybenzo[*d*]isothiazol-3(2*H*)-one-*N*-alkylbenzylamine derivatives with acetylcholinesterase, monoamine oxidases and *β*-amyloid aggregation inhibitory activities as potential agents against Alzheimer's disease

Rui Xu[a,1], Ganyuan Xiao[a,1], Yan Li[a], Hongyan Liu[a], Qing Song[a], Xiaoyu Zhang[a], Ziyi Yang[a], Yunxiaozhu Zheng[a], Zhenghuai Tan[b,*], Yong Deng[a,*]

[a]*Department of Medicinal Chemistry, Key Laboratory of Drug Targeting and Drug Delivery System of the Education Ministry, West China School of Pharmacy, Sichuan University, Chengdu, 610041, China*

[b]*Institute of Traditional Chinese Medicine Pharmacology and Toxicology, Sichuan Academy of Chinese Medicine Sciences, Chengdu 610041, China*

[1] These authors contributed equally to this work.

**Corresponding Author*.

E-mail: tanzhh616@163.com (Zhenghuai Tan)

E-mail: dengyong@scu.edu.cn (Yong Deng)

Abstract

A series of 5,6-dimethoxybenzo[*d*]isothiazol-3(2*H*)-one-*N*-alkylbenzylamine derivatives were designed, synthesized and evaluated as potential multifunctional agents for the treatment of Alzheimer's disease (AD). The *in vitro* assays indicated that most of these derivatives were selective AChE inhibitors with good multifunctional properties. Among them, compounds **11b** and **11d** displayed comprehensive advantages, with good AChE (IC_{50} = 0.29 ± 0.01 μM and 0.46 ± 0.02 μM, respectively), MAO-A (IC_{50} = 8.2 ± 0.08 μM and 7.9 ± 0.07 μM, respectively) and MAO-B (IC_{50} = 20.1 ± 0.16 μM and 43.8 ± 2.0% at 10 μM, respectively) inhibitory activities, moderate self-induced A$\beta_{1\text{-}42}$ aggregation inhibitory potency (35.4 ± 0.42% and 48.0 ± 1.53% at 25 μM, respectively) and potential antioxidant activity. In addition, the two representative compounds displayed high BBB permeability *in vitro*. Taken together, these multifunctional properties make **11b** and **11d** as a promising candidate for the development of efficient drugs against AD.

Keywords:

Alzheimer's disease; Benzo[*d*]isothiazol-3(2*H*)-one derivatives; Monoamine oxidase inhibitors; Acetylcholinesterase inhibitors; Aβ aggregation inhibitors; Multifunctional agents.

1. Introduction

Alzheimer's disease (AD) is a chronic, neurodegenerative, and fatal disease in the brain, characterized by memory loss, behavioral disturbances and many other cognitive impairments.[1] More than 47 million patients suffer from AD currently, and the number is increasing annually.[2] Unfortunately, its mechanism has not been fully elucidated due to complex etiology. Although the exact cause of AD remains elusive, reports suggest the involvement of several factors for the development of the disease, including β-amyloid (Aβ) deposits, oxidative stress, τ-protein aggregation, dyshomeostasis of biometals and low levels of acetylcholine (ACh) in the hippocampus and cortex area of the brain, are considered to play vital roles in the pathophysiology of AD.[3,4]

It has been known that the level of acetylcholine (ACh) receptors is reduced in AD episodes and the dysfunction of cholinergic signal transmission could be responsible for the symptoms of AD.[5] ACh is mainly hydrolyzed by acetylcholinesterase (AChE) at the cholinergic synapses. Hence, FDA has approved several AChE inhibitors for AD treatment including rivastigmine, donepezil (**1**, **Figure 1**), and galantamine. In addition, AChE also accelerates the aggregation of amyloid fibrils, obtaining stable AChE-Aβ complexes, which is thought to involve the peripheral anionic site (PAS) of AChE and is more toxic than single Aβ peptide.[6] Although, it has been proved that the inhibition of butyrylcholinesterase (BuChE) was beneficial for the treatment of AD,[7] but serious inhibition of BuChE may contribute to the potential peripheral side effects of ChE inhibitors (e.g., the dual AChE and BuChE inhibitor, tacrine, which has shown severe hepatotoxicity as well as other adverse effects).[8] Therefore, it may be more rational to design selective AChE inhibitors for AD treatment, with expectation of lower side effects.

Monoamine oxidases (MAOs) have received much attention in recent years for their roles in the treatment of AD. MAOs are flavin adenine dinucleotide (FAD) containing enzymes, which exist as two different isoforms (MAO-A and -B).[9] The enzymes play an important role in the metabolism and regulation of major xenobiotic amine and monoamine neurotransmitters. It is known that AD patients usually present depressive symptoms that may aggravate the development of the disease.[10] MAO-A inhibitors have been shown to be effective antidepressants such as moclobemide and toloxatone, while selective MAO-B inhibitors have been used to treat the neurodegenerative disorders like AD and Parkinson's.[11] Furthermore, the high level of MAO-B was able to lead to an increase in the levels of hydrogen peroxide and oxidative free radicals, which contribute to the etiology of AD. In addition,

several studies have indicated that MAOs increase the expression of γ-secretase and β-secretase and improve Aβ generation from amyloid precursor protein.[12] Therefore, inhibition of MAOs may be of value for AD therapy.

Based on the amyloid hypothesis, aggregation and deposition of Aβ peptide considered to initiate the pathogenic cascade may result in neuronal loss and dementia.[13] Aβ peptide exists as two primary isoforms: A$\beta_{1\text{-}40}$ and A$\beta_{1\text{-}42}$. Among the two isoforms, though the amount of A$\beta_{1\text{-}42}$ is only 10% of A$\beta_{1\text{-}40}$, A$\beta_{1\text{-}42}$ displays a higher tendency to aggregate, lower solubility and stronger neuronal toxicity than A$\beta_{1\text{-}40}$.[14] Hence, preventing the formation and aggregation of A$\beta_{1\text{-}42}$ represents a rational approach for the treatment of AD. In addition, oxidative stress plays a crucial role in neuronal degeneration. According to literature reports that oxidative damage can do harm to biological molecules such as proteins, lipids and DNA.[15] Furthermore, recent studies have shown that oxidative damage could promote the neurofibrillar tangles and appearance of amyloid plaques in AD.[16] So, designing compounds that could clear or prevent the formation of the free radicals is a potential efficient strategy against AD.

Due to the complexity of AD, the current "one-molecule, one-target" paradigm therapeutic drugs seem not so efficient. Therefore, development of drugs with two or more complementary bioactivities for the treatment of AD seems more effective. Considering above, our work is focused on the rational design, synthesis and evaluation of novel multifunctional molecules against AD.

Sulfonamides are important antimicrobial agents that play an important role in the treatment of infectious diseases. The parent structure of sulfonamide has shown a wide range of biological activity after structural modification.[17] For example, sulfonamide derivatives have been reported to display monoamine oxidase inhibitory activity,[18] and the saccharin-*N*-alkylamine derivatives (**2**, **Figure 1**) was an efficient selective AChE inhibitor and showed moderate inhibitory potencies of Aβ aggregation also it has the activities of neuroprotection.[19] The diversities of the bioactivity makes it an excellent leading compound to design new multifunctional agents against AD. Furthermore, the peripheral anionic site (PAS) of AChE is closely related to the aggregation of amyloid fibrils.[6] In order to increase the inhibitory activity of Aβ aggregation, we tried to enhance the π-π stacking between the compound and the PAS of AChE through changing the sulfone group in the mother nucleus to sulfur atom. On the other hand, since the sulfide compound has the function of capturing the free radical, reducing the sulfone group to the sulfur atom may increase the antioxidant activity of

the compound. Moreover, donepezil is the only drug of the five AChE inhibitors currently available that can act simultaneously on the PAS and CAS of AChE.[20-22] Thus, in view of the similarity with the structure of the donepezil and saccharin, we introduce methoxy groups to the 5,6-position of benzo[*d*]isothiazol-3(2*H*)-one moiety. The X-ray crystal structures of the complexes of donepezil and AChE protein showed that the benzyl moiety binds to the CAS via a π-π interaction with Trp84, and the piperidine ring was applied to the hydrophobic part of the channel. In addition, this compound showed π-π stacking with the benzene ring of Phe330 and the hydrogen bond is formed with the water molecule simultaneously, after the nitrogen atom was protonated.[23] Therefore, we combined 5,6-dimethoxybenzo[*d*]isothiazol-3(2*H*)-one with appropriate benzylamine moiety by using different lengths of carbon spacers to design a series of novel 5,6-dimethoxybenzo[*d*]isothiazol-3(2*H*)-one-*N*-alkylbenzylamine derivatives (**Figure 1**), that are expected to act as multifunctional agents with AChE and MAOs inhibitions, anti-A*β* aggregation and antioxidant properties. In addition, to investigate the effect of different oxidation states of sulfur atoms on the biological activity, we also selectively synthesized the 5,6-dimethoxybenzo[*d*]isothiazol-3(2*H*)-one 1-oxide and 1,1-dioxide alkylbenzylamine derivatives.

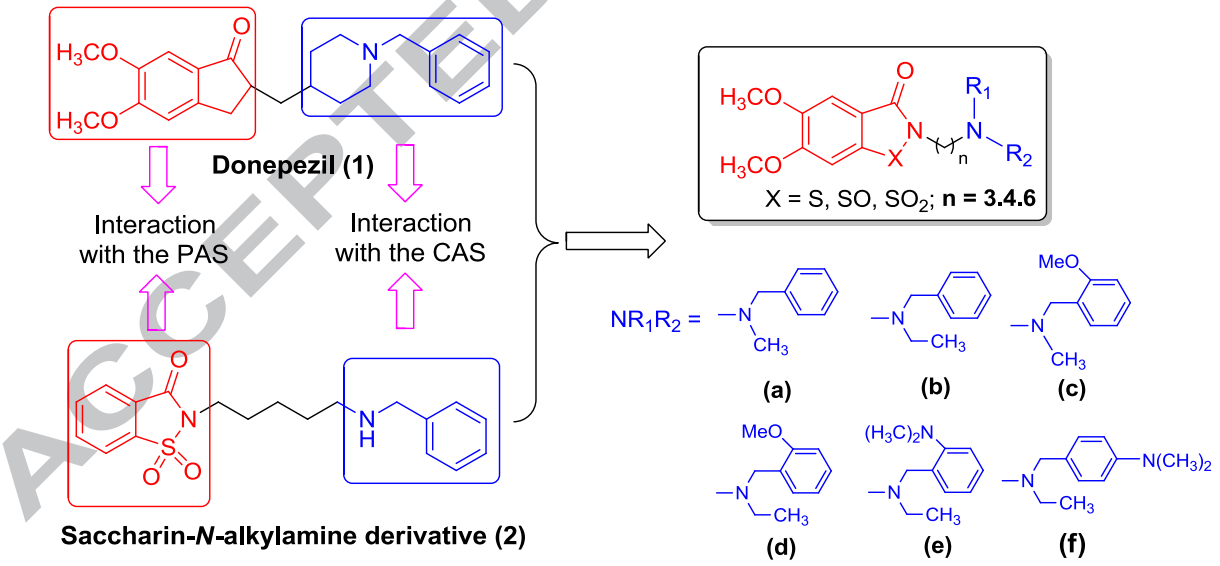

Figure 1. Design strategy for 5,6-dimethoxybenzo[*d*]isothiazol-3(2*H*)-one-*N*-alkylbenzylamine derivatives.

2. Results and discussion

2.1. Chemistry

The synthetic route for the target derivatives were summarized in **Scheme 1**. The 4,4',5,5'-tetramethoxy-2,2'-dithiobis(benzoic acid) (**4**) was obtained by conventional method through Sandmeyer reaction starting from the 2-amino-4,5-dimethoxybenzoic acid.[24] And then intermediate **4** was reacted with $SOCl_2$ at 80 ^oC for 10 h in toluene to afford the compound **5**. Finally, compound **5** was reacted with the corresponding primary amines **6-8**[25] in pyridine at room temperature to afford the target compounds **9-11**. Meanwhile compounds **18** and **19** were obtained from another route. Compound **5** was treated with excessive amounts of NH_4OH to give the compound **12**. Then, the intermediate **12** was oxidized in presence of oxidant H_5IO_6 and catalytic amount of CrO_3[26] to yield intermediates **13** and **14**, respectively. Subsequently, these intermediates were reacted with 1,6-dibromohexane in the presence of anhydrous K_2CO_3 at room temperature to provide the key intermediates **15** and **16**. Finally, the target compounds **18** and **19** were obtained by treatment of intermediates **15** and **16** with corresponding secondary amines NHR_1R_2 (**17**)[25] in CH_3CN under reflux for 5-6 h. All of the target compounds were purified using chromatography, and the analytical and spectroscopic data confirmed their structures, as detailed in the experimental section.

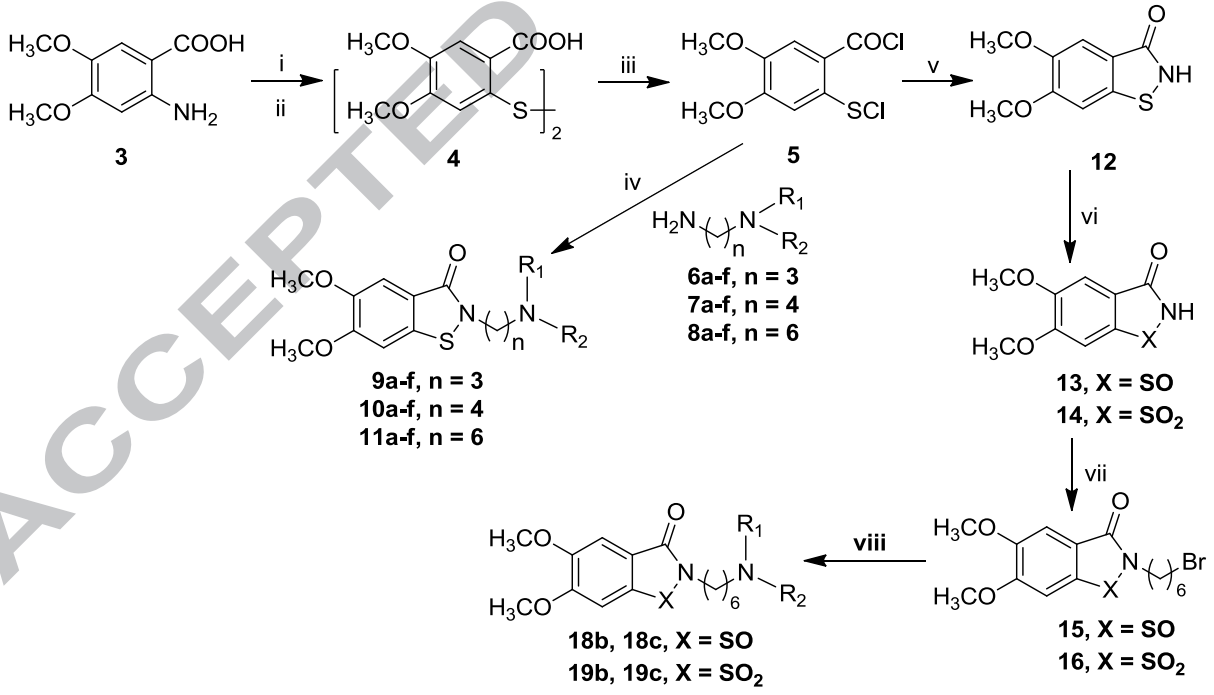

Scheme 1. Synthesis of 5,6-dimethoxybenzo[*d*]isothiazol-3(2*H*)-one-*N*-alkylbenzylamines. *Reagents and conditions*: (i) $NaNO_2$, *conc.* HCl, H_2O, 5 °C for 10 min; (ii) S, $Na_2S{\cdot}9H_2O$, NaOH 0-5 °C, then r.t. for 2 h; (iii) $SOCl_2$, toluene, 80 ^oC for 10 h; (iv) pyridine, CH_2Cl_2, r.t. for 2 days; (v) NH_4OH, pyridine, CH_2Cl_2, r.t. for 2 days; (vi) H_5IO_6/CrO_3, CH_3CN, r.t. for 10 min or reflux for 1h; (vii)

$Br(CH_2)_6Br$, K_2CO_3, DMF, r.t. for overnight; (viii) NHR_1R_2 (**17**), K_2CO_3, CH_3CN, reflux for 5-6 h.

2.2. Pharmacology

2.2.1. Evaluation of AChE and BuChE inhibitory activities

The inhibitory activities of the target compounds against AChE which is from *Electrophorus electricus* (*Ee*AChE) and BuChE which is from rat serum (*Rat*BuChE) were determined by modified Ellman's method.[27,28] Donepezil was used as the reference compound. The results for the inhibition of AChE and BuChE were summarized in **Table 1**. It can be seen from the table that the lead compound **12**, displayed low AChE inhibitory activity (IC_{50} = 34.90 ± 0.02 μM) while all of the target compounds showed significant inhibitory activities with IC_{50} values ranging from 0.21 μM to 13.1 μM. It is showed that the *N*-alkylbenzylamine group was beneficial. Among all of the tested compounds, compound **11b** displayed the most potent *Ee*AChE inhibitory activity (IC_{50} = 0.29 ± 0.01 μM). Moreover, the AChE inhibitory potency was related to the length of alkylene spacer chains. In general, the derivatives with 4- or 6-methylene linker showed better AChE inhibition than those with 3-methylene chain (e.g. **11c** > **10c** > **9c**). The reason may be that the side chain is too short for the compound to act on the CAS and PAS sites of AChE at the same time. It is obvious that **11b** and **11c** exhibited higher inhibitory activity against AChE compared with the **18b**, **18c**, **19b** and **19c**, which the sulfur atom in molecular nucleus was oxidized to sulfoxide or sulfone respectively. On the other hand, this series of compounds demonstrated weak BuChE inhibitory activity, and it can be seen from these data that the compounds are highly selective acetylcholinesterase inhibitors. Since BuChE is predominantly present in the peripheral tissues and in plasma, high selectivity for AChE inhibitory activity may reduce associated side effects. Among them, compounds **11b** exhibited a degree of efficiency to inhibit BuChE (48.2 ± 0.83% at 50 μM).

Table 1. The chemical structures, purity, AChE and BuChE inhibitory activities of intermediate **12**, compounds **9-11**, **18**, **19** and Donepezil.

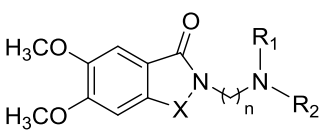

Compd.	X	n	NR_1R_2	Purity (%)	*Ee*AChE IC_{50} (μM)[a]	*Rat*BuChE % Inhibition[b]
12	S	—	—	98.8	34.90 ± 0.02	10.3 ± 0.27

9a	S	3	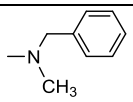	98.3	7.50 ± 0.01	11.5 ± 0.28
9b	S	3	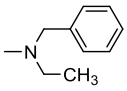	97.9	6.65 ± 0.01	12.3 ± 0.29
9c	S	3	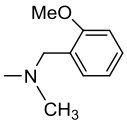	97.6	12.05 ± 0.02	10.8 ± 0.28
9d	S	3	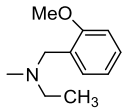	97.2	8.30 ± 0.01	18.9 ± 0.36
9e	S	3	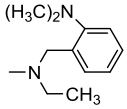	98.4	9.70 ± 0.02	27.9 ± 0.45
9f	S	3	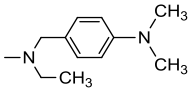	97.5	12.90 ± 0.02	9.6 ± 0.26
10a	S	4	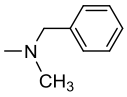	97.3	1.20 ± 0.01	14.7 ± 0.32
10b	S	4	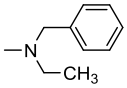	98.6	0.80 ± 0.02	21.8 ± 0.40
10c	S	4	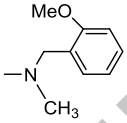	98.7	5.90 ± 0.02	25.5 ± 0.45
10d	S	4	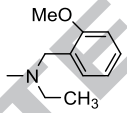	98.7	4.99 ± 0.01	36.4 ± 0.72
10e	S	4	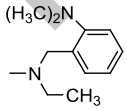	96.9	7.10 ± 0.01	32.6 ± 0.71
10f	S	4	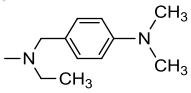	98.1	8.85 ± 0.02	23.2 ± 0.42
11a	S	6	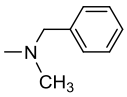	97.6	0.35 ± 0.01	23.1 ± 0.43
11b	S	6	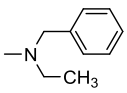	98.6	0.29 ± 0.01	48.2 ± 0.83
11c	S	6	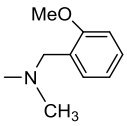	97.3	0.61 ± 0.02	28.8 ± 0.51
11d	S	6	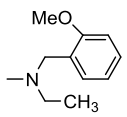	98.3	0.46 ± 0.02	46.9 ± 0.81
11e	S	6	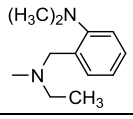	97.5	0.56 ± 0.01	46.8 ± 0.80

11f	S	6	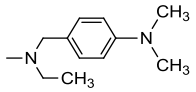	97.5	6.50 ± 0.01	22.7 ± 0.46
18b	SO	6	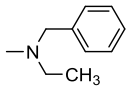	98.4	0.38 ± 0.01	8.1 ± 0.24
18c	SO	6	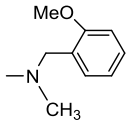	97.8	0.80 ± 0.01	28.7 ± 0.52
19b	SO_2	6	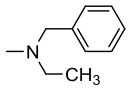	98.2	13.1 ± 0.03	35.7 ± 0.74
19c	SO_2	6	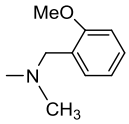	96.8	1.02 ± 0.01	n.a.[c]
Donepezil	—	—	—	—	0.023 ± 0.003	IC_{50} = 21.4 ± 0.097μM

[a] AChE from *Electrophorus electricus*. IC_{50} values represent the concentration of inhibitor required to decrease enzyme activity by 50% and are the mean of three independent experiments, each performed in triplicate. Data were expressed as mean ± SD (SD = standard deviation).

[b] BuChE from rat serum and percentages are the percent inhibition of BuChE by tested compounds at 50 μM.

[c] n.a. = no active. Compounds defined "no active" means a percent inhibition is less than 5.0% at a concentration of 50 μM in the assay conditions.

2.2.2. Kinetic study for the inhibition of AChE

In order to gain further insight into the mechanism of action on AChE of this series of compounds, a kinetic study was carried out on compound **11b** using *Ee*AChE.[27] Graphical analysis of the reciprocal Lineweaver-Burk plots showed that both increasing slopes (decreased V_{max}) and intercepts (higher K_m) at increasing concentration of the inhibitor (**Figure 2**). This pattern revealed a mixed-type inhibition, which implied that compound **11b** was likely to bind both of the CAS and the PAS of AChE.

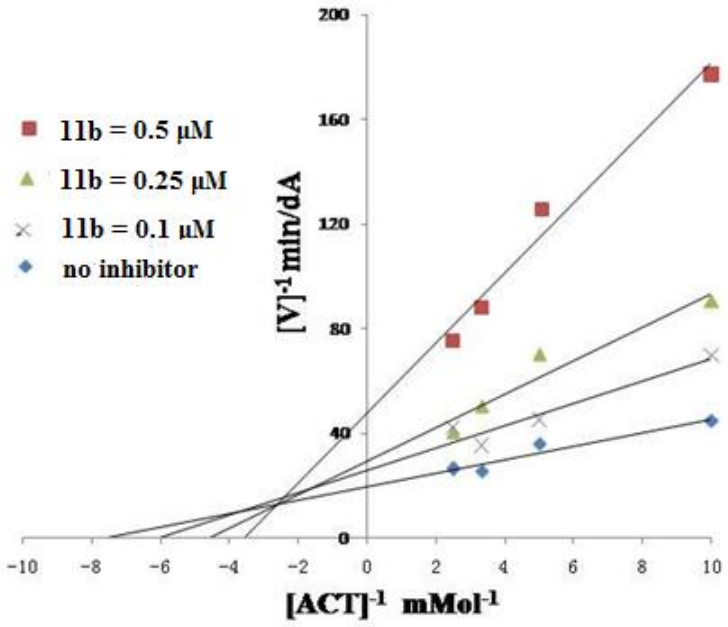

Figure 2. Kinetic study on the mechanism of *Ee*AChE inhibition by compound **11b**. Overlaid Lineweaver-Burk reciprocal plots of AChE initial velocity at increasing substrate concentration (0.1-0.4 mM) in the absence and presence of **11b** are shown. Lines were derived from a weighted least-squares analysis of data points.

2.2.3. Molecular modeling study of AChE and BuChE

To clarify the binding modes of these derivatives with *Tc*AChE (PDB: *1EVE*), docking studies were carried out using the AUTODOCK 4.2 package with Discovery Studio 2.5.[29] Considering the results of AChE inhibition assay and the kinetic study, compound **11b** was chosen for our molecular modeling investigation. The result was shown in **Figure 3**, the compound **11b** occupied the entire enzymatic catalytic active site (CAS), the mid-gorge sites and the peripheral anionic site (PAS). In the *Tc*AChE-**11b** complex, the benzylamine moiety of **11b** was observed to bind to the CAS via a π-π interaction with Tyr130 and potentially induce a hydrophobic interaction with residues Gly441, Trp84, Leu127, Ser124, Glu199, Gly123 and Gly117. The 5,6-dimethoxybenzo[*d*]isothiazol-3-one moiety occupied the PAS of AChE and exhibited a potential hydrophobic interaction with residues Tyr334, Gly335, Ile287, Ser286, Arg289 and Phe290, and the benzene ring of this moiety was observed to adopt parallel π-π interactions with Phe331 and Phe288. The sulfur atom could bind to the Tyr121 via intermolecular hydrogen bonds. In addition, the long chain of methylene folded in a

conformation in the gorge that allowed it to interact with His440、Tyr121、Ser122、Gly118 and Ser200 via the hydrophobic interaction. The docking study indicated that **11b** could bind to the CAS and PAS of AChE and thus revealed a mixed-type inhibition, consistent with our kinetic analysis result. A docking study with BuChE was also performed (**Figure S2**, Supporting Information), and the result indicated that **11b** could not bind to the BuChE as stable as AChE, which would explain the weak BuChE inhibitory potency of our derivatives.

To further elucidate why **18b** displayed the similar AChE inhibitory activities as **11b** while **19b** was different from **11b**, docking studies of **18b** and **19b** were also performed. The overlap of **11b** and **18b** in AChE (**Figure S3**, Supporting Information) indicates that the sulfoxide group does not affect the binding mode, which agrees with the *in vitro* activity assay. The conclusion was similar to the selenium-containing compounds reported in literature.[30] As for **19b**, the molecular docking result showed that there was less interaction of the molecule with AChE than **11b** (**Figure S4**, Supporting Information). In addition, the binding energy and inhibit constant of **19b** were -10.96 kcal/mol and 9.23 nM while the corresponding values of **11b** were -12.02 kcal/mol and 1.54 nM, which may give the reason why the AChE inhibitory activity of **19b** was different from **11b**. And, the overlap of **11b**, **18b** and **19b** in AChE (**Figure S5**, Supporting Information) was also consistent with this result.

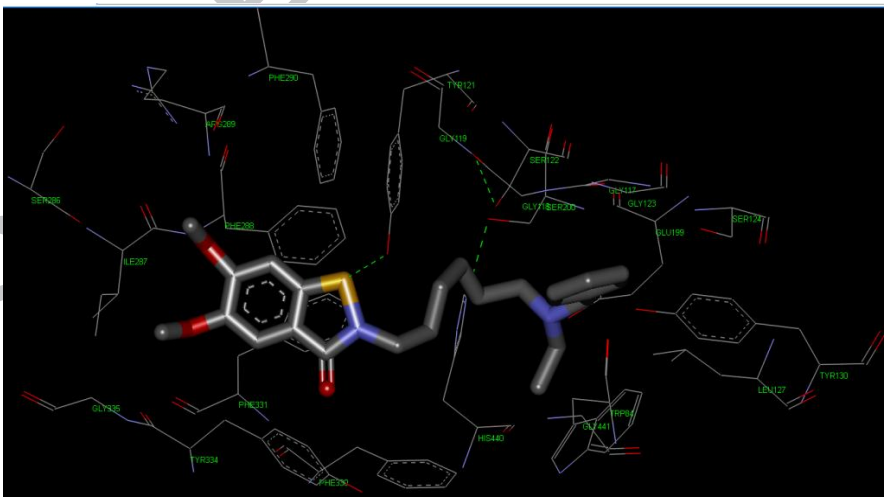

Figure 3. Hypothetical binding mode of compound **11b** (colored by atom type) interacting with residues in the binding site of *Tc*AChE (PDB: *1EVE*). The protein residues that participate in the main interactions with the inhibitor are labeled.

2.2.4. *In vitro* antioxidant activity assay

The antioxidant activities of compounds **9-11**, **12**, **18** and **19** were evaluated by following the

well-established ORAC-FL method,[31,32] and the results were summarized in **Table 2**. Trolox (a water-soluble vitamin E analogue) was used as a standard, and the compounds' ability to scavenge radicals was provided as a Trolox equivalent. It can be seen from the results that most of the target compounds exhibited low to moderate antioxidant activity while compounds **11f**, **10f** and **9a** showed the most potent antioxidant activities of this family with ORAC-FL values of 1.92, 2.14 and 0.91 Trolox equivalents, respectively. Although the effect of different benzylamine substituents on the antioxidant activity did not show a significant structure-activity relationship, the introduction of *N*-(4-dimethylaminobenzyl) ethylamine substituent significantly enhanced the antioxidant activity. However, there was no significant change in antioxidant activity when the target compounds **11b** and **11c** were oxidized to **18b**, **18c**, **19b** and **19c**.

2.2.5. Inhibition of self-induced A$\beta_{1\text{-}42}$ aggregation

To investigate the effects of the derivatives on self-induced A$\beta_{1\text{-}42}$ aggregation, the Thioflavin T (ThT) fluorescence assay was performed, with curcumin as a reference compound.[33,34] The results summarized in **Table 2** indicated that most of the compounds showed moderate to decent inhibitory potencies of self-induced A$\beta_{1\text{-}42}$ aggregation. The compounds with the most potent inhibition effects on self-induced A$\beta_{1\text{-}42}$ aggregation were **10f**, **11b**, **11d**, **11f** and **18c**, with respective inhibition ratio of 32.5 ± 1.33%, 35.4 ± 0.42%, 48.0 ± 1.53%, 33.4 ± 1.23% and 38.0 ± 1.23% at 25 μM. Among them, the inhibitory activity of the compound **11d** (48.0 ± 1.53%) was higher than the reference compound curcumin (41.3 ± 0.9%). Structure-activity relationship analysis indicated that the derivatives with 6-methylene linker showed better inhibition of self-induced A$\beta_{1\text{-}42}$ aggregation than those with 3- or 4-methylene chain except **11a** and **11c**. Besides, when the sulfur atom was oxidized to sulfone or sulfoxide, a regular structure-activity relationship cannot be summarized.

Table 2. *In vitro* inhibition of self-induced A$\beta_{1\text{-}42}$ aggregation, recombinant human MAO-A and -B, and oxygen radical absorbance capacity (ORAC, trolox equivalent) of intermediate **12**, compounds **9-11**, **18**, **19** and reference compounds.

Compd.	ORAC[a]	% Inhibition of self-induced A$\beta_{1\text{-}42}$ aggregation[b, c, f]	IC_{50} ± SD (μM)[d, f]		SI[e]
			MAO-A	MAO-B	
12	0.29 ± 0.03	12.2 ± 1.01	21.0 ± 0.19	14.0% ± 1.1%	—
9a	0.91 ± 0.05	7.6 ± 0.41	6.9 ± 0.06	44.4% ± 2.1%	—

9b	0.84 ± 0.02	19.6 ± 0.31	9.9 ± 0.08	46.3% ± 2.2%	—
9c	0.83 ± 0.03	21.8 ± 1.22	9.4 ± 0.09	48.6% ± 2.4%	—
9d	0.82 ± 0.05	12.4 ± 0.71	15.5 ± 0.05	37.0% ± 1.9%	—
9e	0.22 ± 0.04	19.8 ± 1.02	16.6 ± 0.15	45.4% ± 2.4%	—
9f	0.58 ± 0.05	13.4 ± 0.82	11.3 ± 0.13	40.1% ± 2.0%	—
10a	0.21 ± 0.04	17.3 ± 0.82	8.9 ± 0.12	19.7 ± 0.17	0.45
10b	0.53 ± 0.02	9.4 ± 0.61	19.9 ± 0.17	20.1 ± 0.18	0.99
10c	0.39 ± 0.09	11.7 ± 0.72	7.1 ± 0.10	19.2 ± 0.17	0.37
10d	0.30 ± 0.04	21.1 ± 1.22	9.6 ± 0.10	19.4 ± 0.17	0.49
10e	0.34 ± 0.05	11.7 ± 0.81	9.9 ± 0.11	46.5% ± 2.3%	—
10f	2.14 ±0.13	32.5 ± 1.33	15.9 ± 0.15	18.8 ± 0.15	0.85
11a	0.29 ± 0.04	4.3 ± 0.25	23.0 ± 0.20	13.2 ± 0.13	1.74
11b	0.27 ± 0.02	35.4 ± 0.42	8.2 ± 0.08	20.1 ± 0.16	0.41
11c	0.26 ± 0.01	20.2 ± 0.73	19.9 ± 0.16	13.7 ± 0.14	1.45
11d	0.28 ± 0.02	48.0 ± 1.53	7.9 ± 0.07	43.8% ± 2.0%	—
11e	0.35 ± 0.01	31.2 ± 1.43	3.4 ± 0.03	19.6 ± 0.15	0.17
11f	1.92 ± 0.05	33.4 ± 1.23	7.1 ± 0.06	12.4 ± 0.13	0.57
18b	0.23 ± 0.03	29.2 ± 1.47	21.5% ± 1.2%	14.6% ± 0.9%	—
18c	0.33 ± 0.04	38.0 ± 1.23	23.8% ± 1.3%	12.2% ± 0.7%	—
19b	0.20 ± 0.01	6.0 ± 0.31	30.2% ± 1.6%	38.9% ± 1.8%	—
19c	0.16 ± 0.01	23.9 ± 0.93	28.1% ± 1.4%	29.2% ± 1.5%	—
Curcumin	—	41.3 ± 0.9	—	—	—
Clorgyline	—	—	0.0027± 0.0006	4.19 ± 0.101	0.00064
Rasagiline	—	—	1.42 ± 0.015	0.083 ± 0.002	17.11
Iproniazid	—	—	2.56 ± 0.023	1.95 ± 0.074	1.31
Donepezil	—	n.a.[g]	—	—	—

[a] The mean SD of the 3 independent experiments. Data are expressed as μM of Trolox equivalent/μM of tested compound.

[b] For inhibition of Aβ aggregation, the thioflavin-T fluorescence method was used.

[c] Inhibition of self-induced A$\beta_{1\text{-}42}$ aggregation (25 μM) by tested inhibitors at 25 μM.

[d] Percentages are the percent inhibition of MAOs by tested compounds at 10 μM.

[e] SI = IC_{50} (MAO-A) / IC_{50} (MAO-B).

[f] The mean ± SD of the three independent experiments.

[g] n.a. = no active. Compounds defined "no active" means a percent inhibition is less than 5.0% at a

concentration of 25 μM in the assay conditions.

2.2.6. Recombinant human MAO-A and -B inhibition studies

To complete the study of the multi-target biological profile of the target compounds, their ability to inhibit recombinant human MAO-A and MAO-B was evaluated with the recombinant human MAO-A and -B as the enzyme sources.[35-37] Clorgyline, rasagiline and iproniazid were used as reference compounds. The results were summarized in **Table 2**. In general, most of the derivatives could effectively inhibit MAO-A, retaining the activities of the lead compound **12** (IC_{50} = 21.0 ± 0.19 μM) while only a part of compounds displayed good MAO-B inhibitory activities (IC_{50} value in micromolar range). It could be seen from **Table 2** that the compound **11e** showed significantly inhibitory activity for MAO-A (IC_{50} = 3.4 ± 0.03 μM) while the compound **11f** exhibited the most potent inhibitory activity for MAO-B (IC_{50} = 12.4 ± 0.13 μM). The results of structure-activity relationship analysis showed that the length of the carbon chain of these compounds had a great effect on the inhibitory activity. The derivatives with 6-methylene linker showed better inhibition of MAO-A than those with 3- or 4- methylene chain except **11a** and **11c**. Besides, when the sulfur atom was oxidized to sulfone or sulfoxide, the inhibition of MAOs activity was significantly reduced.

2.2.7. *In vitro* blood-brain barrier permeation assay

The ability to cross the blood-brain barrier (BBB) and reach the therapeutic targets is an important prerequisite for drugs to act on neurodegenerative processes. To evaluate the brain penetration of representative compound **11b** and **11d**, we conducted a parallel artificial membrane permeation assay for the blood-brain barrier (PAMPA-BBB), as recently described by Di *et al.*[38,39] We used 11 commercial drugs to do the experiment and got their permeability then compared with the reported values to validate the assay (**Table S1**, Supporting Information). A plot of experimental data versus the bibliographic values displayed a good linear correlation: P_e (exp.) = 0.9163 × P_e (bibl.) − 0.2247 (R^2 = 0.9558) (**Figure S1**, Supporting Information). From this equation and considering the limit established by Di *et al.* for blood-brain barrier permeation,[38] we determined that compounds with permeability above 3.44 × 10^{-6} cm/s could cross the blood-brain barrier (**Table S2**, Supporting Information).[40] The results presented in **Table 3** showed that compound **11b** and **11d** could penetrate into the CNS with good BBB permeability.

Table 3. Permeability P_e ($\times 10^{-6}$ cm/s) in the PAMPA-BBB assay of the selected compounds **11b** and **11d** with their predictive penetration in the CNS

Compd.[a]	P_e ($\times 10^{-6}$ cm/s)[b]	Prediction
11b	15.58 ± 0.23	CNS +
11d	4.32 ± 0.10	CNS +

[a] Compound **11b** and **11d** were dissolved in DMSO at 5 mg/mL and diluted with PBS/EtOH (70:30). The final concentration of the compounds was 100 μg/mL.

[b] Values are expressed as the mean ± SD of three independent experiments.

3. Conclusion

In summary, the *in vitro* assays showed that most of these derivatives exhibited good AChE inhibitory activities, moderate inhibitory activities of MAOs, moderate to good inhibitory potencies of self-induced A$\beta_{1\text{-}42}$ aggregation and antioxidant activities. Among them, compound **11b** and **11d** displayed comprehensive advantages, with good AChE (IC_{50} = 0. 29 ± 0.01 μM and 0.46 ± 0.02 μM, respectively), MAO-A (IC_{50} = 8.2 ± 0.08 μM and 7.9 ± 0.07 μM, respectively) and MAO-B (IC_{50} = 20.1 ± 0.16 μM and 43.8 ± 2.0% at 10 μM, respectively) inhibitory activities, moderate self-induced A$\beta_{1\text{-}42}$ aggregation inhibitory potency (35.4 ± 0.42% and 48.0 ± 1.53% at 25 μM, respectively) and potential antioxidant activity. In addition, the two representative compounds also displayed high BBB permeability *in vitro*. Taken together, these multifunctional properties make **11b** and **11d** as a promising candidate for the development of efficient drugs against AD.

4. Experimental section

4.1. Chemistry

All chemical reagents and solvents were obtained from commercial sources (without further purification). Melting points were measured in open glass capillaries on YRT-3 melting-point apparatus (China) and uncorrected. ^{1}H NMR and ^{13}C NMR spectra were recorded on a Varian INOVA 600 NMR spectrometer or Varian INOVA 400 NMR spectrometer at room temperature using $CDCl_3$ or DMSO-d_6 as the solvent. Chemical shifts (δ) are reported in ppm from internal Tetramethylsilane (TMS), coupling constants (*J*) are reported in hertz (Hz). Mass spectra were recorded on Agilent-6210 TOF LC-MS Spectrometer. HPLC analysis was carried out on a Shimadzu

LC-10Avp plus system with the use of a Kromasil C_{18} column (4.6 mm × 250 mm, 5 μm). Reactions were monitored by thin-layer chromatography (TLC) using silica gel GF_{254} plates from Qingdao Haiyang Chemical Co. Ltd. (China) and the spots were visualized by UV light (254 nm). Crude products were purified by preparative thin-layer chromatography or column chromatography using silica gel from Qingdao Haiyang Chemical Co. Ltd. (China).

4.1.1. Synthesis of 4,4',5,5'-tetramethoxy-2,2'-dithiobis(benzoic acid) (4)

A solution of 2-amino-4,5-dimethoxybenzoic acid (2 g, 10 mmol) in a mixture of water (10 mL) and concentrated hydrochloric acid (2.52 mL, 25 mmol) was diazotized at 0 °C with a solution of $NaNO_2$ (0.69 g, 10 mmol) in water (4 mL) added dropwise. The solution was stirred 10 min at 0 °C and then added to a solution of Na_2S_2 [prepared by heating $Na_2S{\cdot}9H_2O$ (2.68 g, 11 mmol) and S (344.72 mg, 10.6 mmol) in water (10 mL), treating the yellow clear solution with NaOH (608 mg, 15 mmol) in water (5 mL) and cooling] containing ice. The mixture was allowed to stand for 2 h at room temperature then acidified with *conc.* HCl, and the precipitated crude product was filtered. It was dissolved in a warm solution of Na_2CO_3 and filtered. The filtrate was acidified again with *conc.* HCl. The precipitated product was collected by filtration. Compound **4** was obtained as an off-white solid, 79.7% yield, mp > 220 °C.

4.1.2. Synthesis of 2-chlorosulfenyl-4,5-dimethoxybenzoyl chloride (5)

Compound **4** and $SOCl_2$ (2.52 mL, 25 mmol) were added to toluene (20 mL). The mixture was warmed to 80 °C and stirred for 10 h. After complete reaction, the solvent and the excess $SOCl_2$ was removed under vacuum to give a pale yellow solid. Crude product of compound **5** was obtained and used without further purification.

4.1.3. General procedure for the synthesis of 9-11

To a stirred solution of compound **5** (100 mg, 0.37 mmol) and pyridine (0.06 mL, 0.75 mmol) in CH_2Cl_2 (1 mL), corresponding primary amines **6-8** (0.56 mmol) was added dropwise. The reaction mixture was stirred for 2 d at room temperature. After the reaction was completed, the mixture was concentrated. Then water (10 mL) was added to the residue and the mixture was extracted with ethyl acetate (8 mL × 3). The combined organic phases were washed with saturated aqueous sodium chloride (10 mL), dried over sodium sulfate, filtered and concentrated under reduced pressure to give the crude compound. The obtained residue was purified by preparative thin-layer chromatogram to afford **9-11**.

4.1.3.1. 2-(3-(benzyl(methyl)amino)propyl)-5,6-dimethoxybenzo[d]isothiazol-3(2H)-one (9a)

It was synthesized from intermediate **5** and **6a** according to the general procedure. Elution with petroleum ether/ethyl acetate (2/1) gave **9a** as yellow oils. Yield 57.1%. ^{1}H NMR (600 MHz, $CDCl_3$) δ 7.46-7.41 (m, 2H), 7.40 (s, 1H), 7.35-7.31 (m, 3H), 6.95 (s, 1H), 3.98 (s, 3H), 3.96 (s, 3H), 3.95-3.94 (m, 2H), 3.82 (s, 2H), 2.80-2.72 (m, 2H), 2.42 (s, 3H), 2.26-2.16 (m, 2H). ^{13}C NMR (150 MHz, $CDCl_3$) δ 165.5, 153.6, 148.6, 133.7, 130.3 (2C), 128.9 (2C), 128.8, 116.5 (2C), 106.6, 101.5, 60.3, 56.3, 56.1, 52.9, 41.3, 40.2, 25.4. ESI-MS m/z: 373.2 $[M+H]^+$.

4.1.3.2. 2-(3-(benzyl(ethyl)amino)propyl)-5,6-dimethoxybenzo[d]isothiazol-3(2H)-one (9b)

It was synthesized from intermediate **5** and **6b** according to the general procedure. Elution with petroleum ether/ethyl acetate (2/1) gave **9b** as yellow oils. Yield 47.4%. ^{1}H NMR (400 MHz, $CDCl_3$) δ 7.52-7.46 (m, 2H), 7.39 (s, 1H), 7.34-7.29 (m, 3H), 6.95 (s, 1H), 3.98 (s, 3H), 3.96 (s, 3H), 3.93 (t, J = 6.4 Hz, 2H), 3.91 (s, 2H), 2.96-2.80 (m, 4H), 2.34-2.20 (m, 2H), 1.38-1.22 (m, 3H). ^{13}C NMR (150 MHz, $CDCl_3$) δ 165.4, 153.5, 148.6, 133.6, 130.1 (2C), 128.7 (2C), 128.6, 116.5 (2C), 106.6, 101.5, 56.7, 56.2, 56.1, 49.1, 47.0, 41.4, 25.2, 9.5. ESI-MS m/z: 387.4 $[M+H]^+$.

4.1.3.3. 5,6-dimethoxy-2-(3-((2-methoxybenzyl)(methyl)amino)propyl)benzo[d]isothiazol-3(2H)-one (9c)

It was synthesized from intermediate **5** and **6c** according to the general procedure. Elution with petroleum ether/ethyl acetate (2/1) gave **9c** as yellow oils. Yield 59.4%. ^{1}H NMR (600 MHz, $CDCl_3$) δ 7.42 (d, J = 7.8 Hz, 1H), 7.41 (s, 1H), 7.29 (t, J = 7.2 Hz, 1H), 6.95 (s, 1H), 6.94 (t, J = 7.2 Hz, 1H), 6.88 (d, J = 7.8 Hz, 1H), 3.98 (t, J = 7.2 Hz, 2H), 3.97 (s, 3H), 3.95 (s, 3H), 3.84 (s, 3H), 3.82 (s, 2H), 2.74 (t, J = 7.2 Hz, 2H) , 2.41 (s, 3H), 2.18-2.16 (m, 2H). ^{13}C NMR (150 MHz, $CDCl_3$) δ 165.5, 157.9, 153.6, 148.7, 133.8, 131.9, 129.7, 120.6, 116.9 (2C), 110.6, 106.8, 101.5, 56.3, 56.2, 55.4, 54.3, 53.6, 41.7, 41.1, 26.2. ESI-MS m/z: 403.1 $[M+H]^+$.

4.1.3.4. 2-(3-(ethyl(2-methoxybenzyl)amino)propyl)-5,6-dimethoxybenzo[d]isothiazol-3(2H)-one (9d)

It was synthesized from intermediate **5** and **6d** according to the general procedure. Elution with petroleum ether/ethyl acetate (2/1) gave **9d** as yellow oils. Yield 53.8%. ^{1}H NMR (400 MHz, $CDCl_3$) δ 7.44 (d, J = 7.2 Hz, 1H), 7.41 (s, 1H), 7.23 (t, J = 7.2 Hz, 1H), 6.93 (s, 1H), 6.90 (t, J = 7.2 Hz, 1H), 6.86 (d, J = 7.2 Hz, 1H), 3.97 (s, 3H), 3.95 (s, 3H), 3.91 (t, J = 7.2 Hz, 2H), 3.83 (s, 3H), 3.72 (s, 2H), 2.67-2.62 (m, 4H), 2.04-2.00 (m, 2H), 1.11 (t, J = 6.8 Hz, 3H). ^{13}C NMR (100 MHz, $CDCl_3$) δ 165.2,

157.6, 153.3, 148.4, 133.6, 131.7, 130.6, 128.3, 120.6, 116.9, 110.3, 106.6, 101.3, 56.1, 56.0, 55.2, 50.8, 49.8, 47.4, 42.0, 26.6, 10.9. ESI-MS m/z: 417.2 $[M+H]^+$.

4.1.3.5. 2-(3-((2-(dimethylamino)benzyl)(ethyl)amino)propyl)-5,6-dimethoxybenzo[d]isothiazol-3(2H)-one (9e)

It was synthesized from intermediate **5** and **6e** according to the general procedure. Elution with petroleum ether/ethyl acetate (2/1) gave **9e** as yellow oils. Yield 45.7%. ^{1}H NMR (400 MHz, $CDCl_3$) δ 7.88 (d, J = 6.8 Hz, 1H), 7.38 (s, 1H), 7.30 (t, J = 6.8 Hz, 1H), 7.17 (d, J = 6.8 Hz, 1H), 7.11 (t, J = 6.8 Hz, 1H), 6.98 (s, 1H), 4.22 (s, 2H), 3.98 (s, 3H), 3.95 (s, 3H), 3.94 (t, J = 7.6 Hz, 2H), 2.72-2.65 (m, 4H), 2.63 (s, 6H), 2.40-2.28 (m, 2H), 1.42 (t, J = 7.2 Hz, 3H). ESI-MS m/z: 430.0 $[M+H]^+$.

4.1.3.6. 2-(3-((4-(dimethylamino)benzyl)(ethyl)amino)propyl)-5,6-dimethoxybenzo[d]isothiazol-3(2H)-one (9f)

It was synthesized from intermediate **5** and **6f** according to the general procedure. Elution with petroleum ether/ethyl acetate (2/1) gave **9f** as yellow oils. Yield 61.9%. ^{1}H NMR (600 MHz, $CDCl_3$) δ 7.38 (s, 1H), 7.21 (d, J = 8.4 Hz, 2H), 6.95 (s, 1H), 6.58 (d, J = 8.4 Hz, 2H), 3.96 (s, 3H), 3.93 (s, 3H), 3.91 (t, J = 6.6 Hz, 2H), 3.81 (s, 2H), 2.89 (s, 6H), 2.80-2.74 (m, 4H), 2.24-2.16 (m, 2H), 1.26-1.21 (m, 3H). ^{13}C NMR (150 MHz, $CDCl_3$) δ 165.4, 153.5, 150.4, 148.5, 133.7, 131.0 (2C), 116.7 (2C), 112.2 (2C), 106.7, 101.5, 56.2, 56.1, 56.0, 48.7, 46. 8, 41.6, 40.2 (2C), 25.5, 9.88. ESI-MS m/z: 430.1 $[M+H]^+$.

4.1.3.7. 2-(4-(benzyl(methyl)amino)butyl)-5,6-dimethoxybenzo[d]isothiazol-3(2H)-one (10a)

It was synthesized from intermediate **5** and **7a** according to the general procedure. Elution with petroleum ether/ethyl acetate (2/1) gave **10a** as yellow oils. Yield 58.2%. ^{1}H NMR (400 MHz, $CDCl_3$) δ 7.41 (s, 1H), 7.40-7.28 (m, 5H), 6.95 (s, 1H), 3.97 (s, 3H), 3.95 (s, 3H), 3.88 (t, J = 6.8 Hz, 2H), 3.72 (s, 2H), 2.70-2.61 (m, 2H), 2.35 (s, 3H), 1.83-1.73 (m, 4H). ^{13}C NMR (150 MHz, $CDCl_3$) δ 165.4, 153.5, 148.6, 133.5, 129.7 (2C), 128.5 (2C), 128.0, 117 (2C), 106.8, 101.5, 61.3, 56.3, 56.1, 55.8, 43.2, 41.0, 27.1, 22.9. ESI-MS m/z:387.1 $[M+H]^+$.

4.1.3.8. 2-(4-(benzyl(ethyl)amino)butyl)-5,6-dimethoxybenzo[d]isothiazol-3(2H)-one (10b)

It was synthesized from intermediate **5** and **7b** according to the general procedure. Elution with petroleum ether/ethyl acetate (2/1) gave **10b** as yellow oils. Yield 49.3%. ^{1}H NMR (400 MHz, $CDCl_3$) δ 7.41 (s, 1H), 7.40-7.27 (m, 5H), 6.95 (s, 1H), 3.97 (s, 3H), 3.95 (s, 3H), 3.86 (t, J = 6.8 Hz, 2H), 3.75 (s, 2H), 2.76-2.61 (m, 4H), 1.80-1.69 (m, 4H), 1.21-1.12 (m, 3H). ^{13}C NMR (150 MHz, $CDCl_3$)

δ 165.3, 153.4, 148.5, 133.5, 129.5 (2C), 128.4 (2C), 127.8, 116.9 (2C), 106.7, 101.4, 57.2, 56.2, 56.1, 51.7, 46.9, 43.2, 27.1, 22.5, 10.4. ESI-MS m/z: 401.2 $[M+H]^+$.

4.1.3.9. 5,6-dimethoxy-2-(4-((2-methoxybenzyl)(methyl)amino)butyl)benzo[d]isothiazol-3(2H)-one (10c)

It was synthesized from intermediate **5** and **7c** according to the general procedure. Elution with petroleum ether/ethyl acetate (2/1) gave **10c** as yellow oils. Yield 56.2%. ^{1}H NMR (600 MHz, $CDCl_3$) δ 7.49 (d, J = 7.2 Hz, 1H), 7.40 (s, 1H), 7.34 (t, J = 7.2 Hz, 1H), 6.98 (t, J = 7.2 Hz, 1H), 6.96 (s, 1H), 6.91 (d, J = 7.2 Hz, 1H), 3.97 (s, 3H), 3.95 (s, 3H), 3.89 (t, J = 7.8 Hz, 2H), 3.88 (s, 2H), 3.85 (s, 3H), 2.88-2.81 (m, 2H), 2.50 (s, 3H), 1.90-1.80 (m, 4H). ^{13}C NMR (100 MHz, $CDCl_3$) δ 165.3, 157.8, 153.4, 148.5, 133.5, 132.2, 130.2, 120.7, 116.8 (2C), 110.6, 106.6, 101.4, 56.2, 56.1, 55.4, 55.3, 53.9, 43.1, 40.4, 26.9, 22.1. ESI-MS m/z: 417.2 $[M+H]^+$.

4.1.3.10. 2-(4-(ethyl(2-methoxybenzyl)amino)butyl)-5,6-dimethoxybenzo[d]isothiazol-3(2H)-one (10d)

It was synthesized from intermediate **5** and **7d** according to the general procedure. Elution with petroleum ether/ethyl acetate (2/1) gave **10d** as yellow oils. Yield 52.3%. ^{1}H NMR (400 MHz, $CDCl_3$) δ 7.49 (d, J = 7.2 Hz, 1H), 7.41 (s, 1H), 7.26 (t, J = 7.2 Hz, 1H), 6.95 (t, J = 7.2 Hz, 1H), 6.94 (s, 1H), 6.87 (d, J = 8.0 Hz, 1H), 3.97 (s, 3H), 3.95 (s, 3H), 3.86 (t, J = 7.2 Hz, 2H), 3.83 (s, 3H), 3.78 (s, 2H), 2.74-2.62 (m, 4H), 1.80-1.69 (m, 4H), 1.16 (t, J = 7.2 Hz, 3H). ^{13}C NMR (150 MHz, $CDCl_3$) δ 165.3, 157.7, 153.4, 148.6, 133.5, 131.6, 130.9, 128.7, 120.5, 117.1, 110.3, 106.8, 101.4, 56.3, 56.1, 55.3, 52.2, 50.8, 47.4, 43.5, 27.3, 23.0, 10.8. ESI-MS m/z: 431.0 $[M+H]^+$.

4.1.3.11. 2-(4-((2-(dimethylamino)benzyl)(ethyl)amino)butyl)-5,6-dimethoxybenzo[d]isothiazol-3(2H)-one (10e)

It was synthesized from intermediate **5** and **7e** according to the general procedure. Elution with petroleum ether/ethyl acetate (2/1) gave **10e** as yellow oils. Yield 50.5%. ^{1}H NMR (400 MHz, $CDCl_3$) δ 7.40 (s, 1H), 7.34-7.17 (m, 4H), 6.96 (s, 1H), 4.25 (s, 2H), 3.98 (s, 3H), 3.95 (s, 3H), 3.87 (t, J = 6.8 Hz, 2H), 3.05-2.89 (m, 4H), 2.64 (s, 6H), 1.90-1.77 (m, 4H), 1.36-1.25 (m, 3H). ESI-MS m/z: 444.2 $[M+H]^+$.

4.1.3.12. 2-(4-((4-(dimethylamino)benzyl)(ethyl)amino)butyl)-5,6-dimethoxybenzo[d]isothiazol-3(2H)-one (10f)

It was synthesized from intermediate **5** and **7f** according to the general procedure. Elution with

petroleum ether/ethyl acetate (2/1) gave **10f** as yellow oils. Yield 44.6%. ^{1}H NMR (400 MHz, $CDCl_3$) δ 7.41 (s, 1H), 7.28 (d, J = 8.4 Hz, 2H), 6.96 (s, 1H), 6.67 (d, J = 8.4 Hz, 2H), 3.97 (s, 3H), 3.95 (s, 3H), 3.9-3.83 (m, 2H), 3.82 (s, 2H), 2.95 (s, 6H), 2.84-2.71 (m, 4H), 1.84-1.74 (m, 4H), 1.29-1.21 (m, 3H). ^{13}C NMR (150 MHz, $CDCl_3$) δ 165.5, 153.6, 150.5, 148.7, 133.6, 131.1 (2C), 117.1 (2C), 112.3 (2C), 106.9, 101.5, 56.3 (2C), 56.2, 51.1, 46.5, 43.2, 40.4 (2C), 27.2 (2C), 9.9. ESI-MS m/z: 444.3 $[M+H]^+$.

4.1.3.13. 2-(6-(benzyl(methyl)amino)hexyl)-5,6-dimethoxybenzo[d]isothiazol-3(2H)-one (11a)

It was synthesized from intermediate **5** and **8a** according to the general procedure. Elution with petroleum ether/ethyl acetate (2/1) gave **11a** as yellow oils. Yield 49.4%. ^{1}H NMR (600 MHz, $CDCl_3$) δ 7.58-7.43 (m, 5H), 7.41 (s, 1H), 6.98 (s, 1H), 4.11 (s, 2H), 3.95 (s, 3H), 3.93 (s, 3H), 3.84 (t, J = 7.2 Hz, 2H), 2.89-2.85 (m, 2H), 2.62 (s, 3H), 1.90-1.83 (m, 2H), 1.74-1.72 (m, 2H), 1.40-1.37 (m, 4H). ESI-MS m/z: 415.1 $[M+H]^+$.

4.1.3.14. 2-(6-(benzyl(ethyl)amino)hexyl)-5,6-dimethoxybenzo[d]isothiazol-3(2H)-one (11b)

It was synthesized from intermediate **5** and **8b** according to the general procedure. Elution with petroleum ether/ethyl acetate (2/1) gave **11b** as yellow oils. Yield 53.1%. ^{1}H NMR (400 MHz, $CDCl_3$) δ 7.58-7.41 (m, 5H), 7.40 (s, 1H), 6.97 (s, 1H), 4.06 (s, 2H), 3.97 (s, 3H), 3.95 (s, 3H), 3.86 (t, J = 7.2 Hz, 2H), 2.99-2.92 (m, 2H), 2.87-2.78 (m, 2H), 1.81-1.73 (m, 4H), 1.41 (t, J = 7.2 Hz, 3H), 1.38-1.34 (m, 4H). ^{13}C NMR (100 MHz, $CDCl_3$) δ 165.2, 153.3, 148.4, 133.4, 128.9 (2C), 128.0 (2C), 126.8, 117.2 (2C), 106.7, 101.3, 57.7, 56.1, 56.0, 52.6, 47.0, 43.7, 29.4, 26.8, 26.3, 26.2, 11.2. ESI-MS m/z: 429.2 $[M+H]^+$.

4.1.3.15. 5,6-dimethoxy-2-(6-((2-methoxybenzyl)(methyl)amino)hexyl)benzo[d]isothiazol-3(2H)-one (11c)

It was synthesized from intermediate **5** and **8c** according to the general procedure. Elution with petroleum ether/ethyl acetate (2/1) gave **11c** as yellow oils. Yield 41.2%. ^{1}H NMR (400 MHz, $CDCl_3$) δ 7.44 (d, J = 7.6 Hz, 1H), 7.42 (s, 1H), 7.31 (t, J = 7.6 Hz, 1H), 6.97 (t, J = 7.6 Hz, 1H), 6.96 (s, 1H), 6.90 (d, J = 8.4 Hz, 1H), 3.97 (s, 3H), 3.95 (s, 3H), 3.86 (t, J = 7.2 Hz, 2H), 3.84 (s, 3H), 3.83 (s, 2H), 2.64 (t, J = 7.6 Hz, 2H), 2.41 (s, 3H), 1.77-1.72 (m, 4H), 1.42-1.37 (m, 4H). ^{13}C NMR (100 MHz, $CDCl_3$) δ 165.3, 157.9, 153.4, 148.6, 133.5, 131.9, 129.7, 120.6, 117.2 (2C), 110.6, 106.8, 101.4, 56.4, 56.3, 56.2, 55.4, 54.2, 43.7, 40.9, 29.3, 26.6, 26.1, 25.6. ESI-MS m/z: 445.2 $[M+H]^+$.

4.1.3.16. 2-(6-(ethyl(2-methoxybenzyl)amino)hexyl)-5,6-dimethoxybenzo[d]isothiazol-3(2H)-one

(11d)

It was synthesized from intermediate **5** and **8d** according to the general procedure. Elution with petroleum ether/ethyl acetate (2/1) gave **11d** as yellow oils. Yield 66.1%. ^{1}H NMR (600 MHz, $CDCl_3$) δ 7.47 (d, J = 7.2 Hz, 1H), 7.27 (s, 1H), 7.25 (t, J = 7.2 Hz, 1H), 6.96 (t, J = 7.2 Hz, 1H), 6.95 (s, 1H), 6.86 (d, J = 8.4 Hz, 1H), 4.00 (s, 3H), 3.97 (s, 3H), 3.86 (t, J = 7.2 Hz, 2H), 3.84 (s, 3H), 3.74 (s, 2H), 2.71-2.62 (m, 2H), 2.59-2.51 (m, 2H), 1.75-1.71 (m, 2H), 1.64-1.54 (m, 2H), 1.41-1.30 (m, 4H), 1.17-1.08 (m, 3H). ESI-MS m/z: 459.2 $[M+H]^+$.

4.1.3.17. 2-(6-((2-(dimethylamino)benzyl)(ethyl)amino)hexyl)-5,6-dimethoxybenzo[d]isothiazol-3(2H)-one (11e)

It was synthesized from intermediate **5** and **8e** according to the general procedure. Elution with petroleum ether/ethyl acetate (2/1) gave **11e** as yellow oils. Yield 58.2%. ^{1}H NMR (400 MHz, $CDCl_3$) δ 7.42 (s, 1H), 7.29-7.10 (m, 4H), 6.95 (s, 1H), 4.02 (s, 2H), 3.97 (s, 3H), 3.96 (s, 3H), 3.85 (t, J = 7.2 Hz, 2H), 2.75-2.72 (m, 4H), 2.71 (s, 6H), 1.75-1.64 (m, 4H), 1.40-1.26 (m, 4H), 1.22-1.12 (m, 3H).

4.1.3.18. 2-(6-((4-(dimethylamino)benzyl)(ethyl)amino)hexyl)-5,6-dimethoxybenzo[d]isothiazol-3(2H)-one (11f)

It was synthesized from intermediate **5** and **8f** according to the general procedure. Elution with petroleum ether/ethyl acetate (2/1) gave **11f** as yellow oils. Yield 49.4%. ^{1}H NMR (600 MHz, $CDCl_3$) δ 7.42 (s, 1H), 7.22 (d, J = 8.4 Hz, 2H), 6.95 (s, 1H), 6.69 (d, J = 8.4 Hz, 2H), 3.96 (s, 3H), 3.95 (s, 3H), 3.85 (t, J = 7.2 Hz, 2H), 3.65 (s, 2H), 2.94 (s, 6H), 2.67-2.62 (m, 2H), 2.56-2.51 (m, 2H), 1.75-1.73 (m, 2H), 1.63-1.57 (m, 2H), 1.38-1.26 (m, 4H), 1.14 (t, J = 6.6 Hz, 3H). ^{13}C NMR (150 MHz, $CDCl_3$) δ 165.3, 153.5, 150.1, 148.6, 133.5, 130.5 (2C), 117.3 (2C), 112.4 (2C), 106.9, 101.5, 56.7, 56.3, 56.2, 52.1, 46.6, 43.8, 40.6 (2C), 29.4, 26.8,26.3, 25.6, 10.7. MS m/z: 472.3 $[M+H]^+$.

4.1.4. Synthesis of 5,6-dimethoxybenzo[d]isothiazol-3(2H)-one (12)

To a mixture of compound **5** (1 g, 3.7 mmol) and pyridine (0.6 mL, 7.5 mmol) in CH_2Cl_2 (10 mL), NH_4OH (1.25 mL, 18.5 mmol) was added dropwise. The reaction mixture was stirred for 2 d at room temperature. After the reaction was completed, the mixture was concentrated. Then water (30 mL) was added to the residue and the mixture was extracted with ethyl acetate (30 mL × 3). The combined organic phases were washed with saturated aqueous sodium chloride (30 mL), dried over sodium sulfate, filtered and concentrated under reduced pressure to obtain crude compound. After

purification by chromatography on silica gel, the pure product **12** was obtained, yield 49.2%, mp 228.2-229.7 °C. ^{1}H NMR (400 MHz, DMSO-d_6) δ 11.05 (brs, 1H), 7.50 (s, 1H), 7.35 (s, 1H), 3.85 (s, 3H), 3.82 (s, 3H).

4.1.5. Synthesis of 5,6-dimethoxybenzo[d]isothiazol-3(2H)-one 1-oxide (13)

H_5IO_6 (2.3 g, 10 mmol) was dissolved in CH_3CN (40 mL) by vigorous stirring at room temperature for 30 min, and then CrO_3 (5 mg, 0.05 mmol) was added to the solution. The mixture was stirred at room temperature for 5 min. To this solution was added a solution of **12** (0.5 g, 2.5mmol) in CH_3CN (20 mL) at room temperature. The reaction mixture was stirred at room temperature for 10 min until the oxidation was completed, the mixture was then filtered, and the filter cake was washed with CH_3CN. The filtrate was evaporated to dryness under reduced pressure to give crude compound. Then the crude was purified on a silica gel chromatography to afford compound **13** as off-white solid, yield 70.31%, mp > 230 °C. MS m/z: 228.0 $[M+H]^+$.

4.1.6. Synthesis of 5,6-dimethoxybenzo[d]isothiazol-3(2H)-one 1,1-dioxide (14)

H_5IO_6 (3.45 g, 15 mmol) was dissolved in CH_3CN (40 mL) by vigorous stirring at room temperature for 30 min, and then CrO_3 (25 mg, 0.25 mmol) was added to the solution. The mixture was stirred at room temperature for 5 min. To this solution was added a solution of **12** (0.5 g, 2.5mmol) in CH_3CN (20 mL) at room temperature. The resulting mixture was refluxed for 1 h and then filtered. The filtrate was concentrated under reduced pressure to give crude compound. Then the crude was purified on a silica gel chromatography to afford compound **14** as off-white solid, yield 59.31%, mp > 230 °C. MS m/z: 244.1 $[M+H]^+$.

4.1.7. General procedure for the synthesis of 15 and 16

To a mixture of compound **13** or **14** (2.5 mmol) and anhydrous K_2CO_3 (0.35 g, 2.5 mmol) in DMF (8mL), 1,6-dibromohexane (0.82 mL, 5 mmol) was added dropwise at room temperature and stirred for overnight. After the reaction was completed, the mixture was diluted with water (40 mL), and extracted with ethyl acetate (25 mL × 3). The combined organic phases were washed with saturated aqueous sodium chloride (20 mL), dried over sodium sulfate, filtered and concentrated under reduced pressure to give crude compound. After purification by chromatography on silica gel, the pure product **15** or **16** was obtained.

4.1.7.1. 2-(6-bromohexyl)-5,6-dimethoxybenzo[d]isothiazol-3(2H)-one 1-oxide (15)

It was synthesized from intermediate **13** and 1,6-dibromohexane according to the general

procedure. Elution with petroleum ether/ acetone (30/1) gave **15** as colorless oils. Yield 56.9%. ^{1}H NMR (400 MHz, $CDCl_3$) δ 7.40 (s, 1H), 7.31 (s, 1H), 4.02 (s, 3H), 4.00 (s, 3H), 3.92-3.86 (m, 1H), 3.80-3.75 (m, 1H), 3.41 (t, J = 7.8 Hz, 2H), 1.91-1.79 (m, 4H), 1.55-1.40 (m, 4H).

4.1.7.2. 2-(6-bromohexyl)-5,6-dimethoxybenzo[d]isothiazol-3(2H)-one 1,1-dioxide (16)

It was synthesized from intermediate **14** and 1,6-dibromohexane according to the general procedure. Elution with petroleum ether/ acetone (30/1) gave **16** as colorless oils. Yield 69.4%. ^{1}H NMR (400 MHz, $CDCl_3$) δ 7.41 (s, 1H), 7.30 (s, 1H), 4.03 (s, 3H), 4.01 (s, 3H), 3.75 (t, J = 7.2 Hz, 2H), 3.41 (t, J = 7.2 Hz, 2H), 1.90-1.82 (m, 4H), 1.54-1.41 (m, 4H).

4.1.8. General procedure for the synthesis of 18 and 19

To a mixture of the compound **15** or **16** (0.2 mmol) and anhydrous K_2CO_3 (28 mg, 0.2 mmol) in CH_3CN (3 mL), the corresponding secondary amines **17b-c** (0.3 mmol) were added. The reaction mixture was refluxed for 6-8 h under an argon atmosphere. After the reaction was completed, the solvent was evaporated under reduced pressure. Then water (10 mL) was added to the residue and the mixture was extracted with CH_2Cl_2 (10 mL × 3). The combined organic phases were washed with saturated aqueous sodium chloride (10 mL), dried over sodium sulfate, filtered and concentrated under reduced pressure to give crude compound. The obtained residue was purified by preparative thin-layer chromatogram to afford target compounds **18** or **19**.

4.1.8.1. 2-(6-(benzyl(ethyl)amino)hexyl)-5,6-dimethoxybenzo[d]isothiazol-3(2H)-one 1-oxide (18b)

It was synthesized from intermediate **15** and **17b** according to the general procedure. Elution with petroleum ether/acetone (3/1) gave **18b** as colorless oils. Yield 62.3%. ^{1}H NMR (400 MHz, $CDCl_3$) δ 7.48-7.33 (m, 6H), 7.31 (s, 1H), 4.02 (s, 3H), 4.00 (s, 3H), 3.91-3.84 (m, 2H), 3.74 (s, 2H), 2.90-2.60 (m, 4H), 1.78-1.68 (m, 4H), 1.44-1.32 (m, 4H), 1.29-1.18 (m, 3H). ^{13}C NMR (100 MHz, $CDCl_3$) 165.4, 154.1, 153.2, 138.5, 130.0(2C), 129.0, 128.7, 128.4 (2C), 121.6, 106.9, 106.4, 57.0, 56.6 (2C), 51.8, 46.8, 41.2, 29.2, 26.6, 26.3 (2C), 10.1. HR-ESI-MS: Calcd. for $C_{24}H_{33}N_2O_4S$ $[M+H]^+$: 445.2161, found 445.2155.

4.1.8.2. 5,6-dimethoxy-2-(6-((2-methoxybenzyl)(methyl)amino)hexyl)benzo[d]isothiazol-3(2H) one 1-oxide (18c)

It was synthesized from intermediate **15** and **17c** according to the general procedure. Elution with petroleum ether/ acetone (3/1) gave **18c** as colorless oils. Yield 62.3%. ^{1}H NMR (400 MHz, $CDCl_3$) δ 7.41 (s, 1H), 7.35 (d, J = 7.2 Hz, 1H), 7.30 (s, 1H), 7.25 (t, J = 7.2 Hz, 1H), 6.94 (t, J = 7.6

Hz, 1H), 6.87 (d, *J* = 8.0 Hz, 1H), 4.03 (s, 3H), 4.01 (s, 3H), 3.83 (s, 3H), 3.73 (t, *J* = 7.6 Hz, 2H), 3.59 (s, 2H), 2.50-2.42 (m, 2H), 2.26 (s, 3H), 1.86-1.81 (m, 2H), 1.64-1.57 (m, 2H), 1.46-1.36 (m, 4H). HR-ESI-MS: Calcd. for $C_{24}H_{33}N_2O_5S$ $[M+H]^+$: 461.2110, found 461.2108.

4.1.8.3. 2-(6-(benzyl(ethyl)amino)hexyl)-5,6-dimethoxybenzo[d]isothiazol-3(2H)-one 1,1-dioxide (19b)

It was synthesized from intermediate **16** and **17b** according to the general procedure. Elution with petroleum ether/ acetone (3/1) gave **19b** as colorless oils. Yield 52.3%. ^{1}H NMR (400 MHz, $CDCl_3$) δ 7.41-7.22 (m, 7H), 4.02 (s, 3H), 4.01 (s, 3H), 3.71 (t, *J* = 7.2 Hz, 2H), 3.60 (s, 2H), 2.56-2.54 (m, 2H), 2.48-2.44 (m, 2H), 1.85-1.78 (m, 2H), 1.57-1.48 (m, 2H), 1.42-1.30 (m, 4H), 1.06 (t, *J* = 6.8 Hz, 3H). ^{13}C NMR (100 MHz, $CDCl_3$) 159.1, 154.4, 153.9, 138.4, 130.6, 129.0 (2C), 128.2 (2C), 126.9, 120.8, 105.7, 102.3, 57.7, 56.8, 56.7, 52.6, 47.1, 39.4, 28.4, 26.7, 26.5, 26.3, 11.3. HR-ESI-MS: Calcd. for $C_{24}H_{33}N_2O_5S$ $[M+H]^+$: 461.2110, found 461.2111.

4.1.8.4. 5,6-dimethoxy-2-(6-((2-methoxybenzyl)(methyl)amino)hexyl)benzo[d]isothiazol-3(2H) one 1,1-dioxide (19c)

It was synthesized from intermediate **16** and **17c** according to the general procedure. Elution with petroleum ether/ acetone (3/1) gave **19c** as colorless oils. Yield 59.2%. ^{1}H NMR (400 MHz, $CDCl_3$) δ 7.52 (d, *J* = 7.2 Hz, 1H), 7.41 (s, 1H), 7.37 (t, *J* = 7.2 Hz, 1H), 7.29 (s, 1H), 7.01 (t, *J* = 7.2 Hz, 1H), 6.93 (d, *J* = 8.4 Hz, 1H), 4.03 (s, 3H), 4.01 (s, 3H), 3.87 (s, 3H), 3.74 (t, *J* = 6.8 Hz, 2H), 3.70 (s, 2H), 2.84-2.74 (m, 2H), 2.54 (s, 3H), 1.85-1.82 (m, 4H), 1.42-1.38 (m, 4H). ^{13}C NMR (100 MHz, $CDCl_3$) 159.2, 158.1, 154.5, 154.0, 132.7, 130.6 (2C), 121.0 (2C), 120.8, 110.8, 105.8, 102.3, 56.8, 55.8, 55.5, 53.6, 40.1, 39.2, 29.7, 28.2, 26.4, 26.2, 24.7. HR-ESI-MS: Calcd. for $C_{24}H_{33}N_2O_6S$ $[M+H]^+$: 477.2059, found 477.2058.

4.2. Pharmacology

4.2.1. Inhibition experiments of AChE and BuChE

The modified Ellman's method[40] was performed to assess the inhibitory activity of the compounds toward cholinesterase (AChE and BuChE). Purified AChE derived from *Electrophorus electricus* (Sigma–Aldrich Co.) while BuChE from rat serum. For the measurement of EeAChE inhibition assay, the reaction mixture (100 μL) consisted of phosphate-buffered solution (0.1 mmol/L, pH = 8.0, 40 μL), *Ee*AChE (0.05 U/mL, final concentration, 10 μL), acetylthiocholine iodide (1 mmol/L, 30 μL) (J&K Scientific) and different concentrations of test compounds (20 μL). Then

5,5'-dithiobis-2-nitrobenzoic acid (DTNB, 0.2%, 30 μL) (J&K Scientific) was added. The mixture was incubated at 37 ℃ for 15 min and then detected at 412 nm using Varioskan Flash Multimode Reader (Thermo Scientific). For BuChE inhibition assays, phosphate-buffered solution (0.1 mmol/L, pH = 7.4, 40 μL), butyrylthiocholine iodide (1 mmol/L, 30 μL), 25% serum (10 μL) were used, changes in absorbance were detected at 405 nm. Each concentration was assayed in triplicate and Donepezil was used as the positive drug. IC_{50} values were calculated as the concentration of compound that produces 50% AChE or BuChE activity inhibition.

4.2.2. Kinetic study for the inhibition of AChE

Kinetic study for the inhibition of AChE was conducted based on an established method using purified AChE.[27,41] The assay solution (100 μL) containing 0.1 M phosphate-buffered solution (pH = 8.00), *Ee*AChE (0.5 U/mL), different concentrations of test compounds and 0.2% DTNB was incubated for 15 min at 37°C, then the substrate ATCh (acetylthiocholine iodide) in different concentrations was added to the mixture. Kinetic characterization of the hydrolysis of ATCh catalyzed by *Ee*AChE was done at 412 nm. The parallel control experiments were performed without inhibitor in the assay. The plots were assessed by a weighted least square analysis that assumed the variance of v to be a constant percentage of v for the entire data set. Slopes of these reciprocal plots were then plotted against the concentration of **11b** in a weighted analysis and K_i was determined as the intercept on the negative x-axis.

4.2.3. Molecular modeling study of AChE and BuChE

The crystal structures of AChE complexed with donepezil (code ID: 1EVE) were obtained from the Protein Data Bank after eliminating the original inhibitors and water molecules. Molecular modeling studies were performed using the AUTODOCK 4.2 program. The 3D Structure of compounds was built and performed geometry optimization by molecular mechanics. After removal of hydrogen atoms, addition of Gasteiger charges, assignment of proper atomic types and addition of their atomic charges to skeleton atoms, the further preparation of the inhibitor was accomplished. Autotors was used to define the rotatable bonds in the ligands. Polar hydrogen atoms were added to amino acid residues, and Gasteiger charges were assigned to all atoms of the enzyme by using Autodock Tools (ADT; version 1.5.6). The resulting enzyme structure was used as an input for the AUTOGRID program. AUTOGRID performed a pre-calculated atomic affinity grid maps for each atom type in the ligand, plus an electrostatics map and a separate desolvation map presented in the

substrate molecule. All maps were calculated with 0.375 Å spacing between grid points. The center of the grid box was placed at the center of donepezil with coordinates x = 2.023, y = 63.295, z = 67.062. The dimensions of the active site box were set at 50 × 50 × 50 Å. Flexible ligand docking was performed for the compounds. Apart from the referred parameters above, the other parameters were accepted as default. Each docked system was performed by 100 runs of the AUTODOCK search by the Lamarckian genetic algorithm (LGA). Subsequently, a cluster analysis was performed on the docking results using a root mean square (RMS) tolerance of 1.0. The lowest energy conformation of the highest populated cluster was selected for analysis. Visualizations and graphic manipulations were done by Discovery Studio 2.5 software or Autodock Tools. In addition, the molecular modeling study of BuChE (code ID: 1P0I) was carried out at the same way.

4.2.4. *In vitro* antioxidant activity assay

The oxygen radical absorbance capacity-fluorescein (ORAC-FL) assay was performed to assess the antioxidant activity of our target compounds.[31] All the reaction mixture was prepared in duplicate, and at least three independent assays were performed for each sample. 6-hydroxy-2,5,7,8-tetramethylchromane-2-carboxylic acid (Trolox) and fluorescein (FL) were purchased from TCI (Shanghai) Development and 2,2'-Azobis(amidinopropane) dihydrochloride (AAPH) was purchased from Accela ChemBio Co., Ltd. The reaction was carried out in 75 mM phosphate-buffered solution (pH = 7.4) and the final reaction mixture was 200 μL. 20 μL of Antioxidant and 120 μL of FL (150 nM final concentration) were added into the wells of a black 96-well plate and 6-Hydroxy-2,5,7,8-tetramethylchroman-2-carboxylic acid (Trolox) was used as standard (1-8 μM, final concentration). The mixture was pre-incubated for 15 min at 37 °C, and then 60 μL of AAPH solution (12 mM final concentration) was added rapidly using an autosampler. The fluorescence recorded every minute for 90 min with excitation at 485 nm and emission at 535 nm by Varioskan Flash Multimode Reader (Thermo Scientific). A blank (FL + AAPH) using phosphate buffer instead of antioxidant calibration were carried out in each assay. The fluorescence measurements were normalized to the curve of the blank. The ORAC-FL values calculated as previously described.[27]

4.2.5. Inhibition of self-induced A$\beta_{1\text{-}42}$ aggregation

To investigate the self-induced A$\beta_{1\text{-}42}$ aggregation, a Thioflavin T-based fluorometric assay was performed.[42-44] Thioflavin T (Basic Yellow 1, ThT) was purchased from TCI (Shanghai) Development. β-Amyloid$_{1\text{-}42}$ (A$\beta_{1\text{-}42}$), supplied as trifluoroacetate salt, was purchased from

ChinaPeptides Co., Ltd. Hexafluoro-2-propanol (HFIP) was purchased from Energy Chemical. Experiments were performed by incubating A$\beta_{1\text{-}42}$ dissolved in Hexafluoro-2-propanol (HFIP) (1 mg/mL) for 24 h at room temperature. Subsequently, the solvent was evaporated. Then the HFIP pretreated A$\beta_{1\text{-}42}$ was dissolved in dry DMSO to a final concentration of 200 μM. Solutions of test compounds were prepared in DMSO in 2.5 mM for storage and diluted with phosphate-buffered solution (pH = 7.4) before used. 20 μL of A$\beta_{1\text{-}42}$ (25 μM, final concentration) together with 20 μL of test compounds (25 μM, final concentration) were incubated in 50 mM phosphate-buffered solution (pH = 7.4) for 24 h at 37 °C. Then, 50 mM glycine-NaOH buffer (pH = 8.5) containing 160 μL of 5 μM ThT was added. Fluorescence was measured on a Varioskan Flash Multimode Reader (Thermo Scientific) with excitation and emission wavelengths at 446 nm and 490 nm, respectively. Each assay was run in triplicate. The percent inhibition was calculated by the expression: $(1\text{-}IF_i/IF_c) \times 100$ where IF_i and IF_c are the fluorescence intensities obtained for A$\beta_{1\text{-}42}$ in the presence and in the absence of inhibitors after subtracting the background, respectively.

4.2.6. Recombinant human MAO-A and –B inhibition studies

To evaluate the target compounds' ability to inhibit MAO-A and MAO-B, the fluorimetric method[44,45] was performed with kynuramine as a common substrate and recombinant human MAO-A and –B were purchased from Sigma-Aldrich. All the enzymatic reactions were performed in potassium phosphate buffer (100 mM, pH 7.40, containing KCl 20.2 mM) to a final volume of 500 μL, and contained kynuramine (45 μM for MAO-A and 30 μM for MAO-B), various concentrations of the test inhibitors (0-100 μM) and lower than 4% DMSO as cosolvent. The reactions were started by the addition of the enzyme (7.5 μg/mL) and then incubated at 37 °C for 30 min. The reactions were terminated by the addition of 400 μL NaOH (2 mol/L) and 1000 μL water and the mixtures were centrifuged at 16000 g for 10 min. The activity was determined on a Varioskan Flash Multimode Reader (Thermo Scientific) by measuring the fluorescence of the supernatant with excitation and emission wavelengths at 310 nm and 400 nm, respectively. IC_{50} values were estimated from sigmoidal dose-response curves (graphs of the initial rate of kynuramine oxidation versus the logarithm of inhibitor concentration). Each sigmoidal curve was constructed from six different compound concentrations spanning at least three orders of magnitude. IC_{50} values were determined in triplicate and expressed as mean ± SD.

4.2.7. *In vitro* blood-brain barrier permeation assay

To evaluate the BBB permeability of the compounds, the artificial membrane permeation assay of the blood-brain barrier (PAMPA-BBB) described by Di *et al*[38] was performed. The acceptor plate (PVDF membrane, pore size 0.45 μm, MAIPN4550) and the donor plate (MATRNPS50) were purchased from Millipore. Porcine brain lipid (PBL) was purchased from Avanti Polar Lipids. Filter PDVF membrane units (diameter 25 mm, pore size 0.45 μm) were purchased from Pall Corporation which were used to filter the samples. Compound **11b** and **11d** was dissolved in DMSO diluted 50-fold in PBS/EtOH (70:30) to a final concentration of 100 μg/mL. Then, 350 μL of the compounds solutions (100 μg/mL) were added to the donor wells while the acceptor wells were filled with 200 μL of PBS/EtOH (70:30). The filter membrane was coated with 4 μL PBL in dodecane (20 μg/mL). The acceptor filter plate was put on the donor plate carefully, and they were left undisturbed for 18 h at 25 °C. Subsequently, the two plates were separated and the Varioskan Flash Multimode Reader (Thermo Scientific) was used to determine the concentrations of drug in the donor and acceptor wells. Furthermore, every sample was analyzed at ten wavelengths in four wells and in at least three independent runs. P_e was calculated using the following expression:

$$P_e = -\ln [1 - C_A(t)/C_{equilibrium}]/[A \times (1/V_D + 1/V_A) \times t]$$

$$C_{equilibrium} = [C_D(t) \times V_D + C_A(t) \times V_A]/(V_D + V_A)$$

Where P_e is permeability in the unit of cm/s. $C_D(t)$ is the compound concentration in donor well at time t and $C_A(t)$ is the compound concentration in acceptor well at time t. A is effective filter area and t is the permeation time. V_A is the volume of acceptor well and V_D is the volume of donor well. Results are given as the mean ± SD. In this experiment, 11 quality control drugs of known BBB permeability were included to validate the analysis set.

Acknowledgments

This work was supported in part by the Chinese National Natural Science Foundation (20872099), the Research Fund for the Doctoral Program of Higher Education (20110181110079) and the National Science and Technology Major Project on "Key New Drug Creation and Manufacturing Program" (2013ZX09301304-002).

Supplementary data

Supplementary data associated with this article can be found, in the online version.

References

1. Emmerzaal, T. L.; Kiliaan, A. J.; Gustafson, D. R. *J. Alzheimer's Dis.* **2015**, *43*, 739.

2. Martin, P.; Adelina, C.; Martin, K.; Maëlenn, G.; Maria, K. *World Alzheimer Report.* **2016**, 1-140

3. Schelterns, P.; Feldman, H. *Lancet Neurol*. **2003**, *2*, 539.

4. Cavalli, A.; Bolognesi, M. L.; Minarini, A.; Rosini, M.; Tumiatti, V.; Recanatini, M.; Melchiorre, C. *J. Med. Chem.* **2008**, *51*, 347.

5. Nordberg, A. *Biol. Psychiatry* **2001**, *49*, 200.

6. Bolognesi, M. L.; Andrisano, V.; Bartolini, M.; Banzi, R.; Melchiorre, C. *J. Med. Chem.* **2005**, *48*, 24.

7. Mesulam, M. M.; Guillozet, A.; Shaw, P.; Levey, A.; Duysen, E.; Lockridge, O. *Neuroscience* **2002**, *110*, 627.

8. Liston, D. R.; Nielsen, J. A.; Villalobos, A.; Chapin, D.; Jones, S. B.; Hubbard, S. T.; Shalaby, I. A.; Ramirez, A.; Nason, D.; White, W. F. *Eur. J. Pharmacol.* **2004**, *486*, 9.

9. Wang, C. C.; Billett, E.; Borchert, A.; Kuhn, H.; Ufer, C. *Cell. Mol. Life Sci.* **2013**, *70*, 599.

10. Caraci, F.; Copani, A.; Nicoletti, F.; Drago, F. *Eur. J. Pharmacol.* **2010**, *626*, 64.

11. Patil, P. O.; Bari, S. B.; Firke, S. D.; Deshmukh, P. K.; Donda, S. T.; Patil, D. A. *Bioorg. Med. Chem.* **2013**, *21*, 2434.

12. Cai, Z. Y. *Mol Med Rep.* **2014**, *9*, 1533.

13. Huang, L.; Lu, C. J.; Sun, Y.; Mao, F.; Luo, Z. H.; Su, T.; Jiang, H. L.; Shan, W. J.; Li, X. S. *J. Med. Chem.* **2012**, *55*, 8483.

14. Sharma, A. K.; Pavlova, S. T.; Kim, J.; Finkelstein, D.; Hawco, N. J.; Rath, N. P.; Kim, J.; Mirica, L. M. *J. Am. Chem. Soc.* **2012**, *134*, 6625.

15. Modak, M. A.; Parab, P.; Ghaskadbi, S. S. *Diabetes/Metab. Res. Rev.* **2014**, *30*, 31.

16. Petersen, R. B.; Nunomura, A.; Lee, H. G.; Casadesus, G.; Perry, G.; Smith, M. A.; Zhu, X. *J. Alzheimer's Dis.* **2007**, *11*, 143.

17. Moeker, J., Peat, T. S.; Bornaghi, L. F.; Vullo, D.; Supuran, C. T.; Poulsen, S. A. *J. Med. Chem.* **2014**, *57*, 3522.

18. Tavari, M.; Malan, S. F.; Joubert, J. *Med. Chem. Commun.* **2016**, *7*, 1628.

19. Szałaj, N.; Bajda, M.; Dudek, K.; Brus, B.; Gobec, S.; Malawska, B. *Arch. Pharm.* **2015**, *348*,

556.

20. Cheung, J.; Rudolph, M. J.; Burshteyn, F.; Cassidy, M. S.; Gary, E. N.; Love, J.; Franklin, M. C.; Height, J. J. *J. Med. Chem.* **2012**, *55*, 10282.

21. Xiao, G.; Li, Y.; Qiang, X.; Xu, R.; Zheng, Y.; Cao, Z.; Luo, L.; Yang, X.; Sang, Z.; Su, F.; Deng, Y. *Bioorg. Med. Chem.* **2017**, *25*, 1030.

22. Ismaili, L.; Refouvelet, B.; Benchekroun, M.; Brogi, S.; Brindisi, M.; Gemma, S.; Campiani, G.; Filipic, S.; Agbaba, D.; Esteban, G.; Unzeta, M.; Nikolic, K.; Butini, S.; Marco-Contelles, J. *Prog. Neurobiol.* **2017**, *151*, 4.

23. Kryger, G.; Silman, I.; Sussman, J. *Structure.* **1999**, *7*, 297.

24. Giuseppe, C.; Stefania, B.; Sandra, G.; Vito, N.; Caterina, F.; Bruno, C.; Gianluca, G.; Alfredo, C.; Mara, G.; Tiziana, M.; Patrizia, M.; Assunta, D. C.; Domenico, M.; Nazzareno, S.; Bruno, G.; Antonietta, S.; Massimo, C.; Licia, P.; Orlando, G.; Ornella, T.; Paolo, C. *J. Med. Chem.* **2002**, *45*, 344.

25. Liu, Q.; Qiang, X.; Li, Y. Sang, Z.; Li, Y.; Tan, Z.; Deng, Y. *Bioorg. Med. Chem.* **2015**, *23*, 911.

26. Xu, L.; Cheng, J.; Trudell, M. L. *J. Org. Chem.* **2003**, *68*, 5388.

27. Li, Y.; Qiang, X.; Luo, L.; Li, Y.; Xiao, G.; Tan, Z.; Deng, Y. *Bioorg. Med. Chem.* **2016**, *24*, 2342.

28. Qiang, X.; Sang, Z.; Yuan, W.; Li, Y.; Liu, Q.; Bai, P.; Shi, Y.; Ang, W.; Tan, Z.; Deng, Y. *Eur. J. Med. Chem.* **2014**, *76*, 314.

29. He, Y.; Yao, P. F.; Chen, S. B.; Huang, Z. H.; Huang, S. L.; Tan, J. H.; Li, D.; Gu, L. Q.; Huang, Z. S. *Eur. J. Med. Chem.* **2013**, *63*, 299.

30. Luo, Z.; Sheng, J.; Sun, Y.; Lu, C.; Yan, J.; Liu, A.; Luo, H.; Huang, L.; Li, X. *J. Med. Chem.* **2013**, *56*, 9089.

31. Dávalos, A.; Gómez-Cordovés, C.; Bartolomé, B. *J. Agric. Food Chem.* **2004**, *52*, 48.

32. Maalej, E.; Chabchoub, F.; Oset-Gasque, M. J.; Esquivias-Pérez, M.; González, M. P.; Monjas, L.; Pérez, C.; Ríos, C. D. L.; Rodríguez-Franco, M. I.; Iriepa, I.; Moraleda, I.; Chioua, M.; Romero, A.; Marco-Contelles, J.; Samadi, A. *Eur. J. Med. Chem.* **2012**, *54*, 750.

33. Sang, Z.; Qiang, X.; Li, Y.; Yuan, W.; Liu, Q.; Shi, Y.; Ang, W.; Luo, Y.; Tan, Z.; Deng, Y. *Eur. J. Med. Chem.* **2015**, *94*, 348.

34. Yang, F. S.; Lim, G. P.; Begum, A. N.; Ubeda, O. J.; Simmons, M. R.; Ambegaokar, S. S.; Chen, P. P. P.; Kayed, R.; Glabe, C. G.; Frautschy, S. A.; Cole, G. M. *J. Biol. Chem.* **2005**, *280*, 5892.

35. Legoabe, L. J.; Petzer, A.; Petzer, J. P. *Bioorg. Chem.* **2012**, *45*, 1.

36. Novaroli, L.; Reist, M.; Favre, E.; Carotti, A.; Catto, M.; Carrupt, P. A. *Bioorg. Med. Chem.* **2005**, *13*, 6212.

37. Strydom, B.; Malan, S. F.; Castagnoli, N.; Bergh, J. J.; Petzer, J. P. *Bioorg. Med. Chem.* **2010**, *18*, 1018.

38. Di, L.; Kerns, E. H.; Fan, K.; Mcconnell, O. J.; Carter, G. T. *Eur. J. Med. Chem.* **2003**, *38*, 223.

39. Sang, Z.; Li, Y.; Qiang, X.; Xiao, G.; Liu, Q.; Tan, Z.; Deng, Y. *Bioorg. Med. Chem.* **2015**, *23*, 668.

40. Li, Y.; Qiang, X.; Luo, L.; Yang, X.; Xiao, G.; Zheng, Y.; Cao, Z.; Sang, Z.; Su, F.; Deng, Y. *Bioorg. Med. Chem.* **2017**, *25*, 714.

41. Lu, C.; Zhou, Q.; Yan, J.; Du, Z.; Huang, L.; Li, X. *Eur. J. Med. Chem.* **2013**, *62*, 745.

42. Rosini, M.; Simoni, E.; Bartolini, M. Cavalli, A.; Ceccarini, L.; Pascu, N.; McClymont, D. W.; Tarozzi, A.; Bolognesi, M. L.; Minarini, A.; Tumiatti, V.; Andrisano, V.; Mellor, I. R.; Melchiorre, C. *J. Med. Chem.* **2008**, *51*, 4381.

43. Li, R. S.; Wang, X. B.; Hu, X. J.; Kong, L. Y. *Bioorg Med Chem Lett.* **2013**, *23*, 2636.

44. Luo, L.; Li, Y.; Qiang, X.; Cao, Z.; Xu, R.; Yang, X.; Xiao, G.; Song, Q.; Tan, Z.; Deng, Y. *Bioorg. Med. Chem.* **2017**, *25*, 1997.

45. Li, Y. Qiang, X. M.; Luo, L.; Yang, X.; Xiao, G.; Liu, Q.; Ai J.; Tan, Z.; Deng, Y. *Eur. J. Med. Chem.* **2017**, *126*, 762.

Graphical abstract